Published online 26 November 2010 *Nucleic Acids Research, 2011, Vol. 39, No. 5* ***1933–1942***
doi:10.1093/nar/gkq867

Kinetically governed polymorphism of $d(G_4T_4G_3)$ quadruplexes in K^+ solutions

Iztok Prislan[1], Jurij Lah[1,*], Matija Milanic[2] and Gorazd Vesnaver[1,*]

[1]Faculty of Chemistry and Chemical Technology, Physical Chemistry, University of Ljubljana, Askerceva 5 and [2]Jožef Stefan Institute, Complex Matter, Jamova 39, 1000 Ljubljana, Slovenia

Received July 21, 2010; Revised September 10, 2010; Accepted September 12, 2010

ABSTRACT

It has been generally recognized that understanding the molecular basis of some important cellular processes is hampered by the lack of knowledge of forces that drive spontaneous formation/disruption of G-quadruplex structures in guanine-rich DNA sequences. According to numerous biophysical and structural studies G-quadruplexes may occur in the presence of K^+ and Na^+ ions as polymorphic structures formed in kinetically governed processes. The reported kinetic models suggested to describe this polymorphism should be considered inappropriate since, as a rule, they include bimolecular single-step associations characterized by negative activation energies. In contrast, our approach in studying polymorphic behavior of G-quadruplexes is based on model mechanisms that involve only elementary folding/unfolding transitions and structural conversion steps that are characterized by positive activation energies. Here, we are investigating a complex polymorphism of $d(G_4T_4G_3)$ quadruplexes in K^+ solutions. On the basis of DSC, circular dichroism and UV spectroscopy and polyacrylamide gel electrophoresis experiments we propose a kinetic model that successfully describes the observed thermally induced conformational transitions of $d(G_4T_4G_3)$ quadruplexes in terms of single-step reactions that involve besides single strands also one tetramolecular and three bimolecular quadruplex structures.

INTRODUCTION

It has long been recognized that the single-stranded G-rich oligonucleotides have a propensity to form inter- and intra-molecular quadruplex structures that consist of stacked G-quartets formed by a cyclic coplanar Hoogsteen base pairing of the four participating guanines (1–3). These structures are additionally stabilized by K^+ or Na^+ ions that are selectively bound in the central cavity between the G-quartets. Those formed in the presence of K^+ ions appear to be more stable and more complex than those formed in the presence of Na^+ ions (4,5) and due to higher intracellular concentrations of K^+ ions they are considered to be biologically more relevant than those observed in Na^+ solutions. G-quadruplexes may be formed from one (monomolecular), two (bimolecular) and four (tetramolecular) single strands (6). They are highly polymorphic structures with the strand polarity and glycosidic torsion angles strongly dependent on the nature of the cations, the connecting loops and the capping bases (6–13). The G-rich DNA sequences with the potential to form quadruplexes have been found in a number of important biological processes. Thus, the telomeric G-quadruplex structures that may form at the single-stranded overhangs at the ends of chromosomes appear to be promising anticancer targets since their formation has been found to inhibit the activity of the enzyme telomerase required for the proliferation of ~80% of cancer cells (11,14–19). G-quadruplexes have also been implicated in the control regions of some oncogenes (20,21). Recently, some quadruplex-forming oligonucleotide aptamers able to bind to certain cellular proteins have been found to inhibit proliferation of various cancer cells (22,23) and some of them have already been tested in clinical trials as cancer therapeutics (24).

As pointed out by Lane *et al.* (25) in their excellent review our understanding of thermodynamics and kinetics of G-quadruplex formation is rather limited even for short sequences comprising only three to four G-quartets. The main problem is multiple conformations routinely observed in solution that may undergo kinetically governed interconversions and folding/unfolding transitions. In most structural studies performed on G-quadruplexes, the emphasis has been placed on information obtained from the high-resolution methods of X-ray crystallography and NMR. The results extracted

*To whom correspondence should be addressed. Tel: +381 1 2419 414; Fax: +386 1 2419 425; Email: jurij.lah@fkkt.uni-lj.si
Correspondence may also be addressed to Gorazd Vesnaver. Tel: +381 1 2419 402; Fax: +386 1 2419 425; Email: gorazd.vesnaver@fkkt.uni-lj.si

from these studies, however, may lead to contradictory explanations of the observed presence of multiple G-quadruplex species and their thermodynamic and kinetic properties (26–31). Nevertheless, the information obtained from methods like X-ray crystallography, NMR or mass spectrometry (32) supported by molecular modeling and simulations of G-quadruplexes (33,34) is essential for understanding their behavior at the molecular level. On the other hand, methods commonly used in attempts to assign the topology of G-quadruplexes and determine the thermodynamic and kinetic characteristics of systems containing several G-quadruplex species are based on UV and circular dichroism (CD) spectroscopy and differential scanning calorimetry (DSC) (35–40). A number of studies of G-quadruplexes in Na^+ and K^+ solutions have shown that the G-quadruplex topology in K^+ solutions may differ significantly from the one observed in the presence of Na^+ ions (25,41–44). In addition, the formation of some G-quadruplexes observed in Na^+ and K^+ solutions appears to be a kinetically governed process. As a rule, attempts to describe such formations have been based on kinetic models that are physically unacceptable since they include elementary association steps characterized by a negative activation energy (5,45–47).

Recently, our laboratory has investigated the polymorphism of $d(G_4T_4G_3)$ quadruplexes observed in Na^+ solutions using UV and CD spectroscopy and DSC. A novel kinetic model of their folding/unfolding mechanism that suggests coexistence and inter-conversion of three bimolecular quadruplex structures and one unfolded single-stranded form has been proposed. This model successfully describes the measured thermally induced folding/unfolding transitions of $d(G_4T_4G_3)$ quadruplexes in Na^+ solutions and gives for the first time positive activation energies for all the model-predicted elementary steps, including those describing association of two single strands into bimolecular quadruplex structures (48). To test a wider applicability of such approach we followed in this work the thermally induced folding/unfolding transitions $d(G_4T_4G_3)$ quadruplexes in K^+ solutions and tried to interpret them in terms of a kinetically governed coexistence of several quadruplex structures and their unfolded forms. In other words, the major aim of our study was to find a kinetic model of thermally induced transitions of $d(G_4T_4G_3)$ quadruplexes that contains folding/unfolding pathways in terms of which the observed polymorphism of $d(G_4T_4G_3)$ in K^+ solutions could be described. Here we propose a global model (Figure 1) whose predictions are consistent with a variety of experimental data (DSC, UV and CD spectroscopy, gel electrophoresis) and lead for all the model-predicted elementary kinetic steps to physically acceptable positive activation energies.

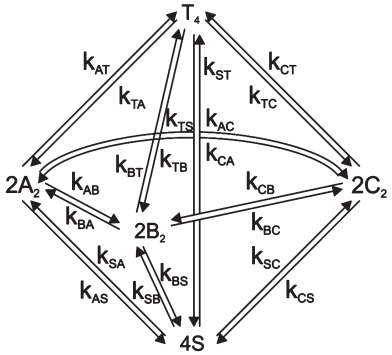

$\Delta H_{AS}=2\bar{H}_S-\bar{H}_A$ $E_{SA}=E_{AS}-\Delta H_{AS}$ $E_{BA}=E_{AB}+\Delta H_{BS}-\Delta H_{AS}$ $E_{TA}=E_{AT}+2\Delta H_{AS}-\Delta H_{TS}$
$\Delta H_{BS}=2\bar{H}_S-\bar{H}_B$ $E_{SB}=E_{BC}-\Delta H_{BS}$ $E_{CB}=E_{BC}+\Delta H_{CS}-\Delta H_{BS}$ $E_{TB}=E_{BT}+2\Delta H_{BS}-\Delta H_{TS}$
$\Delta H_{CS}=2\bar{H}_S-\bar{H}_C$ $E_{SC}=E_{CS}-\Delta H_{CS}$ $E_{CA}=E_{AC}+\Delta H_{CS}-\Delta H_{AS}$ $E_{TC}=E_{CT}+2\Delta H_{CS}-\Delta H_{TS}$
$\Delta H_{TS}=4\bar{H}_S-\bar{H}_T$

$$k_{ij}=e^{A_{ij}-E_{a_{ij}}/RT}$$

Figure 1. Proposed kinetic model for the thermally induced folding/unfolding transitions of $d(G_4T_4G_3)$ in K^+ solutions. It assumes coexistence and interconversions of one tetramolecular quadruplex T_4, three bimolecular quadruplexes A_2, B_2 and C_2 and the unfolded single strands S. $\bar{H}_T$, $\bar{H}_A$, $\bar{H}_B$, $\bar{H}_C$ and $\bar{H}_S$ are the corresponding partial molar enthalpies while k_{ij} are rate constants for each i→j transition step expressed according to Arrhenius in terms of reaction frequency factor $e^{A_{ij}}$ and activation energy E_{ij}.

MATERIALS AND METHODS

Sample preparation

The $d(G_4T_4G_3)$ oligonucleotide was obtained HPLC pure from Invitrogen Co., Germany and Midland Co., USA. and used without further purification. Its concentrations in buffer solutions were determined at 25°C spectrophotometrically using for the extinction coefficient of its single-stranded form at 25°C the value of ε_{260} = 105 100/M/cm estimated from the nearest-neighbor data of Cantor *et al*. (49). The buffer used in all experiments consisted of 10 mM K-cacodylic buffer, 1 mM EDTA and 15 mM KCl (pH = 6.9). The starting samples were first transformed into single-stranded form by heating in an outer thermostat at 95°C for 5 min, cooled down to 4°C at the cooling rates of 0.05 or 1.0°C/min to form quadruplex structures and then used in the UV, CD, DSC and polyacrylamide gel electrophoresis (PAGE) experiments.

UV melting experiments

Absorbance versus temperature profiles of $d(G_4T_4G_3)$ samples were measured in 0.25 mm path-length cells using a Cary 100 BIO UV/Visible Spectrophotometer (Varian Inc.) equipped with a thermoelectric temperature controller. Thermally induced folding/unfolding transitions of $d(G_4T_4G_3)$ quadruplex samples (c ~0.75 mM in single strands) prepared either at the cooling rate of 0.05 or 1.0°C/min were monitored between 5 and 95°C at λ = 298 nm at the heating rate of 1.0°C/min.

Gel electrophoresis

G-quadruplex structures formed upon cooling of single-stranded DNA (~300 μM in 10 μl of 10 mM K-cacodylic buffer, 1 mM EDTA and 15 mM KCl) at the cooling rate of 0.05 or 1.0°C/min were studied by non-denaturing PAGE performed on 20% polyacrylamide gels supplemented with 25 mM KCl. G-quadruplex samples prepared at either of the cooling rates were

loaded on gels and the electrophoreses were run at 5°C (5 h), 10°C (4.5 h), 15°C (4 h) and 20°C (3.5 h), all at 10 V/cm (I = 300 mA). Bands in the gels were followed by UV shadowing at λ = 254 nm. To facilitate comparisons between the bands observed with different samples the single-stranded d(5′-TCTTTTCTTCT-3′) and heteroduplex (5′-AGAAGAAAAGA-3′; 5′-TCTTTTCTT CT-3′) 11-mere control oligonucleotides were used.

DSC

DSC experiments were performed using a Nano DSC II instrument (Calorimetry Sciences Corp., UT, USA) on samples prepared by cooling in an outer thermostat. Quadruplex concentration used in these DSC studies was 0.75 mM in single strands. Cyclic DSC measurements were performed at the heating rates of 0.5, 1.0 and 2.0°C/min and a single cooling rate of 1.0°C/min. Thus, only the first melting scans reflected thermal transitions of samples prepared in the outer thermostat by annealing to 4°C at the cooling rate of 0.05 or 1.0°C/min, while all the following scans were performed on samples prepared in the DSC cell within the cooling cycles at the rate of 1.0°C/min. The measured temperature interval was between 4°C and 95°C. The corresponding baseline (buffer–buffer) scans were subtracted from the unfolding/folding scans prior to their normalization and analysis. The total enthalpy of unfolding or folding, ΔH_{tot}, was obtained from the measured DSC thermograms as the area under the $\Delta C_P = \bar{C}_{P,2} - \bar{C}_{P,S}$ versus T curve, where $\bar{C}_{P,2}$ is the measured heat capacity C_P corrected for the baseline and normalized to 1 mol of quadruplex in single strands and $\bar{C}_{P,S}$ is the corresponding partial molar heat capacity of the unfolded single-stranded state extrapolated from high temperatures over the whole measured temperature interval (Figure 2). For samples prepared either at the cooling rate of 0.05 or 1.0°C/min the measured DSC heating and cooling curves were highly reproducible at all measured heating and cooling rates except for heating curves measured at the rate of 2.0°C/min. At this heating rate the DSC instrument enables reliable measurements only above ~10°C and since the observed low-temperature transitions start occurring below this temperature the reproducibility and reliability of the measured DSC peaks between 4°C and ~20°C is rather poor. To ascertain that the low-temperature peaks observed at all heating rates used in the DSC measurements are real we repeated the described DSC melting experiments on the same samples in another type of DSC instrument (VP-Capillary DSC, MicroCal, USA). Similar melting thermograms containing well expressed low-temperature peaks were obtained thus indicating that the observed appearance of a stable $d(G_4T_4G_3)$ quadruplex structure below ~20°C is not an artifact.

CD Spectroscopy

CD spectra of $d(G_4T_4G_3)$ quadruplexes in K^+ solutions were measured as a function of temperature in an AVIV CD Spectropolarimeter 62A DS, equipped with a thermoelectric temperature controller. Ellipticity, Θ, was measured between 5°C and 95°C in the temperature intervals of 3°C at the average heating rate of 1.0°C/min. CD spectra of samples (~0.75 mM in single strands) prepared at either of the cooling rates, corrected for the corresponding buffer contribution, were collected between 215 and 320 nm in a 0.25-mm cuvette at 60 nm/min, signal averaging time of 2 s and 5 nm bandwidth.

RESULTS AND DISCUSSION

Polymorphism as a kinetic phenomenon

Monitoring the thermally induced folding/unfolding transitions of $d(G_4T_4G_3)$ quadruplexes in 25 mM K^+ solutions by UV absorption spectroscopy resulted in melting profiles that depend on heating and cooling rates and have a shape characteristic of a simple two-state transition. They show hysteresis of UV melting and annealing curves (Supplementary Figure S1) similar to the one reported for $d(G_4T_4G_3)$ and $d(G_4T_4G_4)$ quadruplexes in the presence of Na^+ ions (46,48). Similar was also the result of our attempt to describe the measured UV melting and annealing curves in terms of a simple two-state kinetic model. Negative activation energy obtained for the model-predicted association step, in which upon cooling two single strands associate into the bimolecular quadruplex structure, clearly shows that in K^+ solutions too, the simple two-state kinetic model of thermally induced folding/unfolding transitions of $d(G_4T_4G_3)$ quadruplexes cannot be applied (48).

In contrast to the observed single-step pattern of UV melting and annealing curves the DSC heating and cooling thermograms measured with the $d(G_4T_4G_3)$ starting samples prepared in 25 mM K^+ solutions at the cooling rate of either 0.05 or 1.0°C/min clearly show that the measured melting processes consist of several conformational transitions (Figure 2). For samples prepared in an outer thermostat at the cooling rate of 1.0°C/min the first and all the following melting scans are identical. At all measured heating rates they are characterized by two well expressed melting peaks (at 20 and 45°C) which means that in the measured unfolding process at least two quadruplex structures are involved. By contrast, samples prepared in an outer thermostat at the cooling rate of 0.05°C/min are characterized by first melting scans that at all heating rates consist of three well expressed peaks (at ~20, ~45 and ~65°C) thus indicating the presence of at least three quadruplex structures. All the following scans (cooling rate in repeating loops is 1°C/min), however, contain only two well expressed melting peaks (at ~20 and ~45°C) that are practically identical to the corresponding scans observed with samples prepared at the cooling rate of 1°C/min. Evidently, the number of significantly populated quadruplex species in solution depends strongly on the cooling rate at which they were formed. These results together with the observed shifting of DSC peaks with the increased heating rates to higher temperatures (Figure 2) strongly suggest that the measured conformational transitions are kinetically governed processes. In other words, the overall thermal folding/unfolding transition of $d(G_4T_4G_3)$ in the

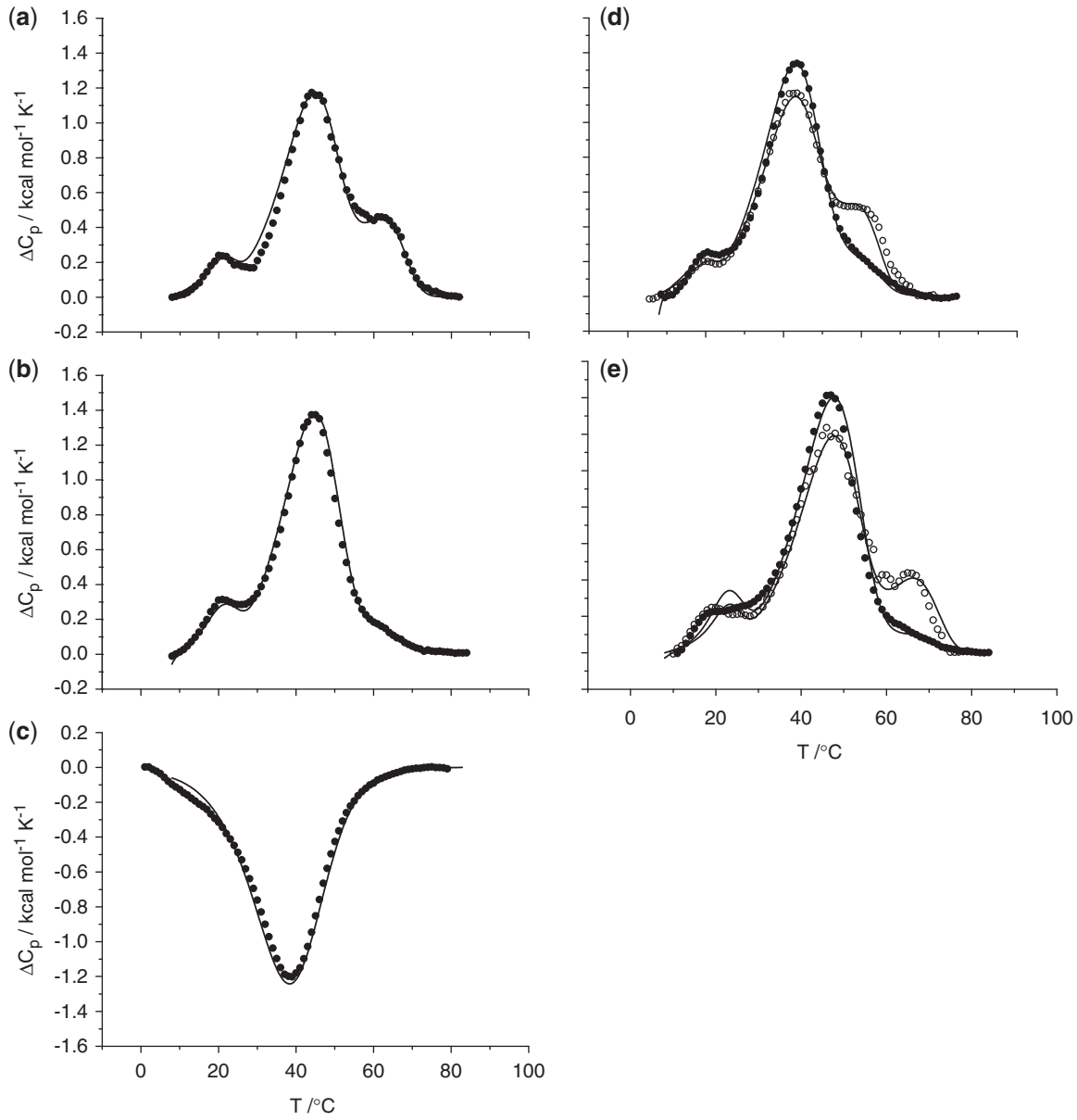

Figure 2. DSC thermograms of $d(G_4T_4G_3)$ quadruplexes in the presence of 25 mM K^+ ions. For clarity reasons every 11th experimental point is shown. The ΔC_p (per mol of single strands) versus T curves: (**a** and **b**) measured at the heating rate of 1°C/min for quadruplex samples prepared at the cooling rate of either 0.05°C/min (a) or 1.0°C/min (b); (**c**) measured at the cooling rate of 1°C/min; (**d** and **e**) measured at the heating rate of 0.5°C/min (**d**) and 2.0°C/min (e) for samples prepared at the cooling rate of either 0.05°C/min (open circles) or 1.0°C/min (filled circles). In all panels full lines represent the corresponding model-based ΔC_p versus T curves calculated from Equation (2) using a single set of the 'best fit' adjustable parameters (Table 1).

presence of K^+ ions may be considered as a combination of several kinetically governed steps. Analysis of the measured DSC thermograms further shows that changes in the cooling rate at which the starting quadruplex samples were prepared and changes in the heating rate at which they were thermally unfolded result only in minor changes in the total area under the measured DSC thermograms (around ±5%). This implies that in K^+ solutions the measured enthalpies of unfolding of different quadruplex structures involved in the unfolding process expressed per mole of single strands are rather close and thus similar to the corresponding overall enthalpy of unfolding, ΔH_{tot}, determined from the total area under the measured DSC thermogram (Figure 2). It should be noted that from these ΔH_{tot} values the enthalpy of quadruplex unfolding is estimated to be ~20 kcal/mol of G-quartets which agrees well with the literature values reported for G-quartet formation in the presence of K^+ ions (50–53).

In line with the conclusions based on the described DSC measurements, gel migration experiments reveal a coexistence of two fast migrating and one slow migrating structural forms (Figure 3). Their contents evidently depend on the cooling rate at which the samples are

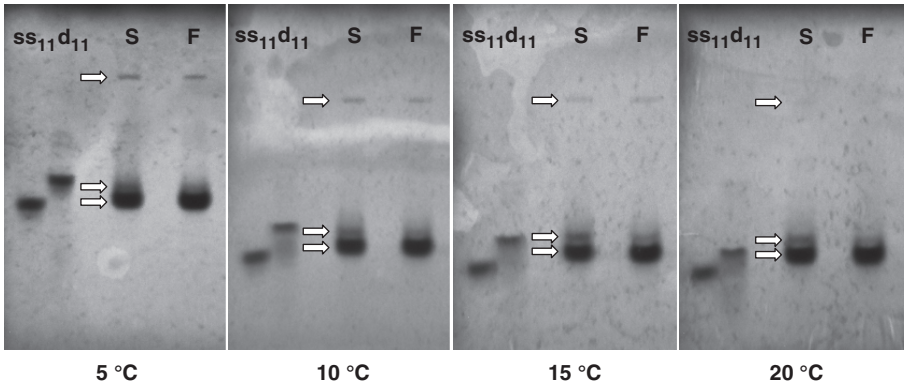

Figure 3. Non denaturing PAGE (20%) experiments. d($G_4T_4G_3$) quadruplexes were prepared at the cooling rate of either 0.05°C/min (**S**) or 1°C/min (**F**) and followed by UV shadowing ($\lambda = 254$ nm) at the constant temperature of 5, 10, 15 and 20°C. As control oligonucleotide 11-mer single-stranded d(5′-TCTTTTCTTCT-3′) and double-stranded d(5′-AGAAGAAAAGA-3′; 5′-TCTTTTCTTCT-3′) markers ss_{11} and d_{11}, were used.

prepared and on the temperature at which the gel migration is performed. The two fast migrating bands that migrate between the single-stranded and heteroduplex 11-mer control oligonucleotide markers may be ascribed to the parallel, anti parallel and/or hybrid bimolecular $d(G_4T_4G_3)_2$ quadruplexes (54), while the much slower migrating band that obviously corresponds to some highly ordered structure may be assumed to originate from the next simplest highly ordered structure, that is, the parallel tetramolecular $d(G_4T_4G_3)_4$ quadruplex. The observed dependence of gel migration on the cooling rate at which the quadruplex structures were formed and on the temperature at which PAGE experiments were conducted is fully consistent with the results of the DSC experiments. Namely, the gel migration experiments run at 5, 10, 15 and 20°C show that between 5°C and 20°C, the intensity of the slowest migrating band and thus the content of the assumed tetramolecular quadruplex structure decreases with increasing temperature. At ~20°C, as shown in Figure 3, the slowest migrating band can no longer be observed indicating that at this temperature the amount of the suggested tetramolecular quadruplexes becomes negligible. This result is in full qualitative agreement with the results of the corresponding DSC experiments which show that the lowest temperature transitions observed with the quadruplex samples prepared at the slow or moderate cooling rates are completed at ~20°C (Figure 2). It seems that the tetramolecular quadruplex is thermally the least stable species, most likely due to its much higher favorable entropy of unfolding (55). The gel electrophoresis experiments also show that samples prepared at the cooling rate of 0.05°C/min are characterized by a more pronounced slower of the two fast migrating bands thus indicating that a higher proportion of the corresponding bimolecular quadruplex structure is very likely responsible for the third observed peak in the corresponding DSC thermograms.

To obtain additional information on the occurrence and transformation of different structures of d($G_4T_4G_3$) quadruplexes during their thermal folding/unfolding transitions, we followed these events also by CD spectroscopy. It should be noted that CD has been used extensively to investigate quadruplex structure of nucleic acids inspite of the fact that there is no simple relationship between the structure of the quadruplex and the shape of its CD spectrum. Numerous publications have reported that folded quadruplex structures of the antiparallel type exhibit CD spectra characterized by a positive ellipticity maximum at ~295 nm and a negative minimum at ~264 nm while those of the parallel type have a positive maximum at ~264 nm and a negative minimum at ~240 nm (54,56–58). Recent studies have shown, however, that so called hybrid quadruplex structures exhibit CD spectra with two positive peaks; one at ~264 nm, typical of a parallel structure and one at ~295 nm, typical of an antiparallel structure. Thus, the appearance of these two peaks, the ratio of which often depends highly on the nature of cations present in the solution (Na^+, K^+), indicates that in the measured thermally induced folding/unfolding transitions besides the parallel and anti parallel structures also the hybrid quadruplex structures may be involved (9,26,27). In other words, all one can follow in quadruplex solutions by CD spectroscopy through the measured peak positions and their magnitudes are changes in the quadruplex topology and not the quadruplex structures themselves. In this work we measured the temperature dependence of CD spectra of d($G_4T_4G_3$) quadruplex samples in K^+ solutions prepared by annealing at the cooling rate of 0.05 and 1.0°C/min. As shown in Figure 4 this dependence differs substantially from the one observed with equally prepared samples in the presence of Na^+ ions (42) whose CD spectra display characteristics of an antiparallel quadruplex topology manifested in a positive band at 295 nm followed by a negative band at 264 nm. In contrast, in K^+ solutions positive peaks at 295 and 264 nm of comparable magnitude are observed (Figure 4) thus indicating the possible presence of parallel, anti parallel and hybrid type of quadruplex structures. Since the two characteristic positive peaks at 295 and 264 nm are present throughout the entire unfolding process it seems reasonable to assume that in the measured thermal unfolding of d($G_4T_4G_3$) quadruplexes the hybrid bimolecular quadruplex structures are strongly involved.

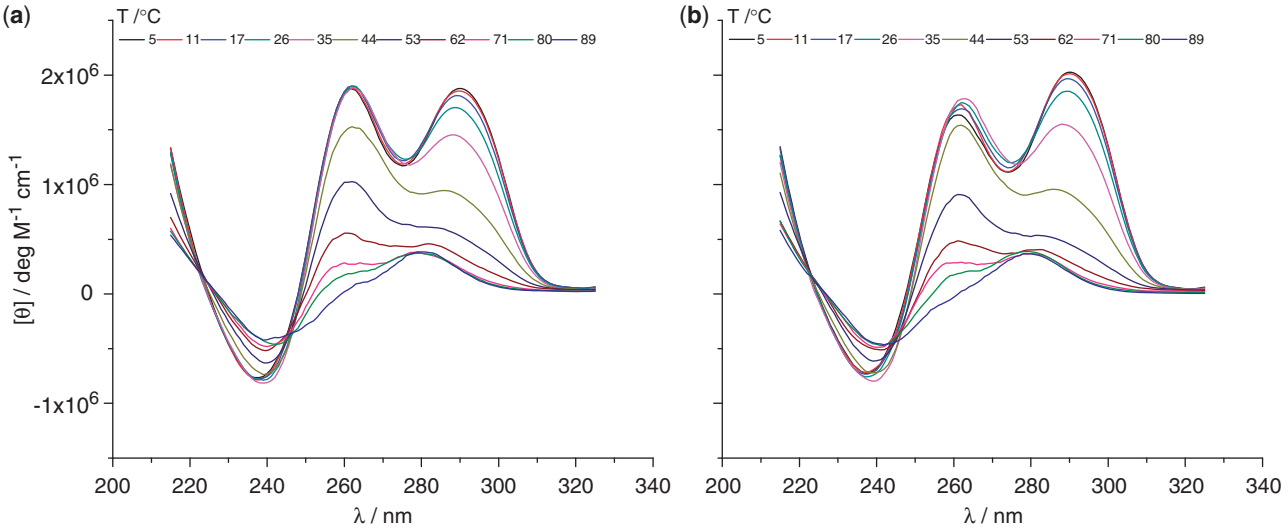

Figure 4. Temperature dependence of CD spectra. d($G_4T_4G_3$) quadruplexes in K^+ solutions (25 mM) were prepared at the cooling rate of either 0.05°C/min (**a**) or 1°C/min (**b**). The measured ellipticity was normalized to 1 M single strand concentration and 1 cm light path length.

In addition, the observed constant positive peak at 264 nm and simultaneous significant drop of the 295-nm positive peak with increasing temperature between ~4 and ~35°C show that at low temperatures unfolding of quadruplex structures other than the bimolecular hybrid quadruplexes takes place. According to PAGE experiments one of these is very likely the assumed slow migrating tetramolecular quadruplex.

Model analysis of structural transitions

The results of DSC, PAGE and CD experiments performed on d($G_4T_4G_3$) quadruplexes in K^+ solutions reveal that their kinetically governed thermally induced folding/unfolding transitions include participation of at least three quadruplex structures. Thus, in our attempts to describe quantitatively the DSC melting and cooling thermograms of d($G_4T_4G_3$) quadruplexes measured at different heating and cooling rates we started first with the kinetic model of the transition process that involves one tetramolecular and two bimolecular quadruplex structures. Unfortunately, a thorough analysis of fitting the corresponding model function to the experimental DSC data has shown that this model fails to describe all the measured DSC thermograms simultaneously in terms of only a single set of adjustable parameters. For this reason, we attempted to interpret the observed DSC data in terms of a new, slightly more complex model (Figure 1), which considers the thermally induced folding/unfolding transitions of d($G_4T_4G_3$) quadruplexes in the presence of K^+ ions as a global kinetic transition process that involves one parallel tetramolecular quadruplex structure (T_4), three bimolecular quadruplexes that possibly exhibit characteristics of parallel, anti parallel and/or hybrid structures (A_2, B_2 and C_2) and the corresponding single strands (S). According to the model the enthalpy, H, of the solution containing n_1 moles of solvent and n_2 moles of DNA (total number n_2 expressed in single-stranded form) can be expressed as (48)

$$H = n_1\bar{H}_1 + n_2\bar{H}_2 = n_1\bar{H}_1 - 2n_A\Delta H_A - 2n_B\Delta H_B - 2n_C\Delta H_C - 4n_T\Delta H_T + n_2\bar{H}_S \quad (1)$$

where the quantities $\Delta H_A = \Delta H_{AS}/2 = \bar{H}_S - \bar{H}_A/2$, $\Delta H_B = \Delta H_{BS}/2 = \bar{H}_S - \bar{H}_B/2$, $\Delta H_C = \Delta H_{CS}/2 = \bar{H}_S - \bar{H}_C/2$ and $\Delta H_T = \Delta H_{TS}/4 = \bar{H}_S - \bar{H}_T/4$ are the enthalpies of unfolding of the quadruplex structures A_2, B_2, C_2 and T_4 into single strands expressed per mole of single strands, n_A, n_B, n_C, n_T and n_S are the numbers of moles of bimolecular quadruplexes A_2, B_2, C_2, tetramolecular quadruplex T_4 and the single-stranded unfolded structure S interrelated as $n_S = n_2 - (2n_A + 2n_B + 2n_C + 4n_T)$ and $\bar{H}_1$, $\bar{H}_A$, $\bar{H}_B$, $\bar{H}_C$, $\bar{H}_T$ and $\bar{H}_S$ are the corresponding partial molar enthalpies. By taking the temperature derivatives of Equation (1) and by assuming that in the measured temperature intervals the heat capacity changes accompanying the unfolding transitions are negligibly small one obtains for the model function, ΔC_P, needed to describe the DSC data, an expression

$$\Delta C_P = \bar{C}_{P,2} - \bar{C}_{P,S} = -\frac{d\alpha_A}{dT}\Delta H_A - \frac{d\alpha_B}{dT}\Delta H_B - \frac{d\alpha_C}{dT}\Delta H_C - \frac{d\alpha_T}{dT}\Delta H_T \quad (2)$$

in which at any T in the measured temperature interval $\bar{C}_{P,2}$ is the measured partial molar heat capacity of the solute (DNA) expressed per moles of single strands, $\bar{C}_{P,S}$ is the corresponding measured heat capacity of the unfolded quadruplex form occurring at high temperatures extrapolated to T and α_A, α_B, α_C and α_T are the corresponding fractions of quadruplex species present in the solution defined as $\alpha_A = 2n_A/n_2$, $\alpha_B = 2n_B/n_2$, $\alpha_C = 2n_C/n_2$ and $\alpha_T = 2n_T/n_2$. Since the enthalpies of unfolding of G-quadruplexes depend primarily on the number of G-quartets involved (50–53) one may assume that for bimolecular quadruplexes (three G-quartets involved) $\Delta H_A = \Delta H_B = \Delta H_C$ while for the parallel

tetramolecular quadruplex (seven G-quartets involved) $\Delta H_T = 7/6\Delta H_A$ or ΔH_B or ΔH_C. Thus, the measured ΔH_{tot} can be expressed as $\Delta H_{tot} = \Delta H_A(1+\alpha_T/6)$ which means that for reasonably low initial α_T values ($\alpha_T \leq 0.3$) one may assume that within an error of 5% $\Delta H_A = \Delta H_B = \Delta H_C = \Delta H_{tot}$ and $\Delta H_T = 7/6\Delta H_{tot}$. Using these estimates, the quantity ΔC_P [Equation (2)] can be calculated at any temperature from the model as $\Delta C_P = -\frac{d\alpha_A}{dT}\Delta H_A - \frac{d\alpha_B}{dT}\Delta H_B - \frac{d\alpha_C}{dT}\Delta H_C - \frac{d\alpha_T}{dT}\Delta H_T$ and compared to the corresponding ΔC_P obtained experimentally as $\Delta C_P = \bar{C}_{P,2} - \bar{C}_{P,S}$. For a given total concentration of DNA in the single-stranded form, c_{tot} expressed as $c_{tot} = c_S+2c_A+2c_B+2c_C+4c_T$ the $d\alpha/dT$ terms needed to calculate ΔC_P are obtained by taking into account the rates of reactions predicted by the model (Figure 1) and the heating or cooling rate, $r = dT/dt$, at which the DSC experiment is performed. By introducing, for each rate constant, k_{ij}, the corresponding Arrhenius relation $k_{ij} = e^{(A_{ij}-E_{ij}/RT)}$ ($e^{A_{ij}}$ frequency factor, E_{ij} activation energy) one obtains (48):

$$
\begin{aligned}
-\frac{d\alpha_A}{dT} &= \frac{1}{r}\left[(k_{AB}+k_{AS}+k_{AC})\alpha_A + c_{tot}k_{AT}\alpha_A^2 - k_{BA}\alpha_B - k_{TA}\alpha_T\right.\\
&\quad \left. -k_{CA}\alpha_C - 2k_{SA}c_{tot}(1-\alpha_A-\alpha_B-\alpha_C-\alpha_T)^2\right]\\
-\frac{d\alpha_B}{dT} &= \frac{1}{r}\left[(k_{BS}+k_{BC}+k_{BA})\alpha_B + c_{tot}k_{BT}\alpha_B^2 - k_{AB}\alpha_A - k_{TB}\alpha_T\right.\\
&\quad \left. -k_{CB}\alpha_C - 2k_{SB}c_{tot}(1-\alpha_A-\alpha_B-\alpha_C-\alpha_T)^2\right]\\
-\frac{d\alpha_C}{dT} &= \frac{1}{r}\left[(k_{CB}+k_{CS}+k_{CA})\alpha_C + c_{tot}k_{CT}\alpha_C^2 - k_{BC}\alpha_B - k_{TC}\alpha_T\right.\\
&\quad \left. -k_{AC}\alpha_A - 2k_{SC}c_{tot}(1-\alpha_A-\alpha_B-\alpha_C-\alpha_T)^2\right]\\
-\frac{d\alpha_T}{dT} &= \frac{1}{r}\left[(k_{TA}+k_{TB}+k_{TC}+k_{TS})\alpha_T - c_{tot}k_{AT}\alpha_A^2 - c_{tot}k_{BT}\alpha_B^2\right.\\
&\quad \left. -c_{tot}k_{CT}\alpha_C^2 - 4k_{ST}c_{tot}^3(1-\alpha_A-\alpha_B-\alpha_C-\alpha_T)^4\right]
\end{aligned}
\tag{3}
$$

To solve this system of differential equations for a given set of adjustable parameters at each measured heating and cooling rate the Cash–Karp adaptive step-size controlled Runge–Kutta method was employed (59) and the obtained solutions (α_i and $d\alpha_i/dT$) were used to calculate the corresponding model function. The 'best fit' adjustable parameters were obtained from global fitting these calculated model functions to the experimental ΔC_P versus T curves using the non-linear minimization of the corresponding χ^2 function [(48) and Supplementary Data S2]. The values of adjustable parameters at the global minimum of χ^2 are considered to be the best descriptors of the experimental ΔC_P versus T curve and, therefore, they are used to characterize the kinetics and thermodynamics of all steps in the suggested model mechanism (Figure 1).

In Figure 2 is presented the best global fit (60) of the model function [Equation (2)] to the DSC heating and cooling curves measured at different heating (0.5, 1.0 and 2.0°C/min) and cooling (1.0°C/min) rates for the quadruplex samples prepared at a very slow (0.05°C/min) or moderate (1.0°C/min) cooling rate. Reasonably good agreement of the model function with the corresponding DSC heating and cooling curves was observed at all measured heating and cooling rates using a single set of 'the best fit' adjustable parameters (Figure 2). Analysis of the applied fitting procedure shows that the lowest possible number of these 'best fit' parameters is obtained when in the suggested reaction mechanism (Figure 1) the steps $S\rightarrow A_2$, $S\rightarrow C_2$, $S\rightarrow T_4$, $A_2\rightarrow T_4$, $T_4\rightarrow A_2$, $C_2\rightarrow T_4$, $T_4\rightarrow C_2$, $T_4\rightarrow B_2$, $C_2\rightarrow B_2$, $A_2\rightarrow C_2$, $C_2\rightarrow A_2$ are assumed to be infinitely slow (the corresponding frequency factors, $e^{A_{ij}}$, are taken as zero). Consequently, for describing the thermally induced folding/unfolding transitions of $d(G_4T_4G_3)$ quadruplexes, we suggest the mechanism presented in Figure 1 in which the above mentioned steps are closed. For this mechanism, the analysis of the adequacy of the applied global fitting procedure (Supplementary Data S3) shows that for each adjustable parameter at its 'best fit' value the χ^2 function exhibits a rather sharp minimum and that for all reactions occurring in the suggested folding/unfolding mechanism the activation energies have physically acceptable positive values (Table 1). It also shows that the correlation between most of the adjustable parameters is rather small, higher correlation is observed only between the frequency factors and the corresponding activation energies (Supplementary Data S3). The errors in adjustable parameters, calculated as square roots of diagonal elements of variance–covariance matrix obtained from fitting the model function [Equation (2)] to the corresponding DSC thermograms, are unreasonably low. This is because they refer only to the quality of fitting to a given set of DSC

Table 1. 'Best Fit' adjustable parameters A_{ij} (unit of $e^{A_{ij}}$ is s^{-1} for unfolding and s^{-1} M^{-1} for folding transitions) and E_{ij} (cal/mol) describing the thermally induced folding/unfolding transitions of $d(G_4T_4G_3)$ quadruplexes in K^+ solutions (25 mM) in terms of the kinetic model presented in Figure 1 together with the corresponding experimentally determined enthalpies of transition, ΔH (cal/mol single strands)

Calculated values	
Parameter	Value and error
A_{BS}	74 ± 5
A_{SB}	19 ± 3
A_{AS}	49 ± 2
A_{TS}	100 ± 10
A_{CS}	54 ± 2
A_{BA}	15.5 ± 0.8
A_{AB}	7.2 ± 0.4
A_{BT}	66 ± 4
A_{BC}	24 ± 2
E_{BS}	$(3.9 \pm 0.2) \times 10^4$
E_{AS}	$(3.2 \pm 0.1) \times 10^4$
E_{TS}	$(6.0 \pm 0.2) \times 10^4$
E_{CS}	$(3.7 \pm 0.1) \times 10^4$
E_{BA}	$(7.0 \pm 0.5) \times 10^3$
E_{BT}	$(3.2 \pm 0.1) \times 10^4$
E_{BC}	$(1.5 \pm 0.1) \times 10^4$
Experimentally determined values	
ΔH_A	$(3.1 \pm 0.2) \times 10^4$
ΔH_B	$(3.1 \pm 0.2) \times 10^4$
ΔH_C	$(3.1 \pm 0.2) \times 10^4$
ΔH_T	$(3.6 \pm 0.2) \times 10^4$

curves and they do not reflect the reliability of the measured DSC curves themselves. Evidently, to obtain more realistic estimation of errors in adjustable parameters one has to take into account the source of the largest error accompanying the DSC measurements in dilute solutions which is undoubtedly the choice of the baseline. Thus, a repetitive evaluation of each measured DSC curve was made using besides the chosen baseline two other baselines, one leading to ΔH_{tot} higher for 5% and one leading to ΔH_{tot} lower for 5% than the reported ΔH_{tot} value based on the chosen baseline. The model function [Equation (2)] was fitted to the resulting ΔC_P versus T curves as described earlier. Then, the obtained different sets of the 'best fit' adjustable parameters were compared and for each parameter the absolute error was estimated as the largest difference of its values appearing in these different sets. The estimated errors of adjustable parameters A_{ij} and E_{ij} are presented in (Table 1).

Tests of the quality of fitting performed individually on the reported 'best fit' adjustable parameters showed for each parameter that introducing of the corresponding estimated error (Table 1) results in a noticeably poorer agreement between the model function and the experiment (Supplementary Figure S2). Poorer agreement was observed also when the highly correlated A_{ij} and E_{ij} adjustable parameters contained in the corresponding rate constants, k_{ij}, were varied simultaneously for the $\pm\Delta A_{ij}$ and $\pm\Delta E_{ij}$ values reported in Table 1 (Supplementary Figure S2). This suggests that within the estimated error margins the observed higher correlation between these complementary parameters A_{ij} and E_{ij} (Supplementary Table S1) has no significant effect on their reliability. In addition, the reliability of the adjustable parameters was also tested by the statistical analysis based on the Monte–Carlo sampling. Using the same limiting error estimates of the DSC baselines as described above, we obtained the parameter errors smaller than those presented in Table 1 (Supplementary Data S3). Thus, according to the discussed analysis one may conclude that the measured DSC thermograms can be reasonably well described in terms of a single set of adjustable parameters originating from the suggested model mechanism (Figure 1 and Table 1).

For each species participating in this mechanism the reported set of adjustable parameters (Table 1) allows estimation of its population at a given oligonucleotide concentration as a function of temperature, the cooling rate at which the quadruplex samples were prepared and the heating rate at which their thermal unfolding was induced (Figure 5). In other words, the measured DSC thermograms of $d(G_4T_4G_3)$ quadruplexes in K^+ solutions may be interpreted in terms of the model-predicted temperature dependence of populations of three bimolecular and one tetramolecular quadruplex structures involved in the measured folding/unfolding process. Interestingly, for the suggested bimolecular quadruplex structure B_2 such calculated population turns out to be negligibly small at all measured temperatures. In other words, the structure B_2 participating in the suggested reaction mechanism (Figure 1) occurs in the measured temperature interval as an extremely unstable intermediate. Consequently, at the measured oligonucleotide concentration (0.75 mM) the only well detectable bimolecular quadruplex structures at low temperatures appear to be A_2 and C_2, with the population of A_2 ($\alpha_A \sim 80\%$) being much higher than that of C_2. As shown in Figure 5 their thermal stabilities are significantly higher than the one ascribed to the tertramolecular quadruplex structure T_4 whose low-temperature population is only ~10%. Furthermore, from the comparison of the calculated structural

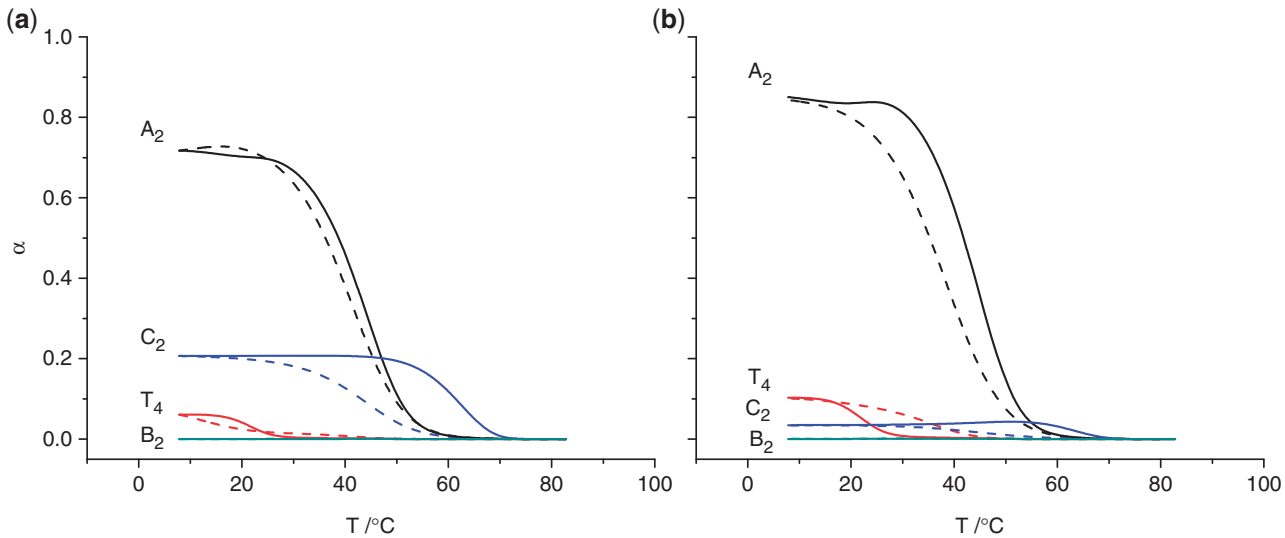

Figure 5. Distribution functions. Distribution of species A_2, B_2, C_2 and T_4 predicted by the model (Figure 1) as a function of temperature for $d(G_4T_4G_3)$ quadruplexes in K^+ solutions (25 mM) calculated from Equation (3) using the 'best fit' adjustable parameters (Table 1). (**a**) formation of structures A_2, B_2, C_2 and T_4 upon cooling (dashed line) at 0.05°C/min and unfolding of these structures upon heating (solid line) at 1°C/min. (**b**) formation of structures A_2, B_2, C_2 and T_4 upon cooling (dashed line) at 1.0°C/min and unfolding of these structures upon heating (solid line) at 1°C/min.

populations involved in the folding/unfolding transitions of $d(G_4T_4G_3)$ followed by DSC ($\alpha_A \sim 80\%$) with the corresponding measured CD spectra (Figure 4) which show throughout the whole thermal unfolding process a strong presence of a hybrid bimolecular $d(G_4T_4G_3)$ quadruplex structure (positive peaks at 295 and 264 nm) one may conclude that A_2 is this structure. Unfortunately, from this comparison one cannot obtain any reliable information about the model-predicted quadruplex structure C_2. Namely, since according to the model, the unfolding of C_2 takes place in the highest temperature interval in which no minimum in CD spectra at 264 nm is observed, all one can conclude is that C_2 is either a parallel or a hybrid quadruplex structure. Finally, since the molecularity of the dimer and tetramer formation is different one would expect the populations of species formed upon cooling to depend on the oligonucleotide concentration. Model-based simulation of the population distribution at 25°C shows, however, that for the total single strand concentration of $d(G_4T_4G_3)$ between 0.5 and 2 mM the calculated changes in population are rather small (Supplementary Figure S3).

In summary, this study demonstrates that the thermally induced formation/disruption of polymorphic $d(G_4T_4G_3)$ quadruplex structures in K^+ solutions is directly related to the cooling/heating rates at which these structures undergo folding/unfolding transitions. Kinetics and thermodynamics of these transitions have been discussed in terms of the simplest physically acceptable model mechanism able to explain the results of DSC (quantitatively) and PAGE and CD (qualitatively) experiments. In discussing the DSC results a detailed model analysis has shown that all 'best fit' adjustable parameters contained in the model function [Equation (2)] are reliable within about $\pm 5\%$. Thus, the suggested kinetic model may be considered realistic and successful. We believe it provides new insights into how individual elementary steps that participate in the folding/unfolding processes and involve polymorphic quadruplex structures may be interrelated through their kinetics and thermodynamics and how they may govern the global folding/unfolding events. Here we show again (48) that any study involving bimolecular and/or tetramolecular G-quadruplex samples should take into account a possibility that the structural composition of these samples depends significantly on the cooling rate at which they are prepared and on the temperature at which they are studied.

SUPPLEMENTARY DATA

Supplementary Data are available at NAR Online.

FUNDING

Slovenian Research Agency through the Grant No. P1-0201; European Cooperation in Science and Technology (COST) action MP0802. Funding for open access charge: Slovenian Research Agency.

Conflict of interest statement. None declared.

REFERENCES

1. Gellert,M., Lipsett,M.N. and Davies,D.R. (1962) Helix formation by guanylic acid. *Proc. Natl Acad. Sci. USA*, **48**, 2013–2018.
2. Arnott,S., Chandrasekaran,R. and Marttila,C.M. (1974) Structures for polyinosinic acid and polyguanylic acid. *Biochem J.*, **141**, 537–543.
3. Sasisekharan,V., Zimmerman,S. and Davies,D.R. (1975) The structure of helical 5′-guanosine monophosphate. *J. Mol. Biol.*, **92**, 171–174.
4. Sen,D. and Gilbert,W. (1990) A sodium-potassium switch in the formation of four-stranded G4-DNA. *Nature*, **344**, 410–414.
5. Mergny,J.-L., De Cian,A., Ghelab,A., Saccà,B. and Lacroix,L. (2005) Kinetics of tetramolecular quadruplexes. *Nucleic Acids Res.*, **33**, 81–94.
6. Burge,S., Parkinson,G.N., Hazel,P., Todd,A.K. and Neidle,S. (2006) Quadruplex DNA: sequence, topology and structure. *Nucleic Acids Res.*, **34**, 5402–5415.
7. Simonsson,T. (2001) G-quadruplex DNA structures–variations on a theme. *Biol. Chem.*, **382**, 621–628.
8. Neidle,S. and Balasubramanian,S. (2006) *Quadruplex Nucleic Acids*. RSC Publishing, Cambridge, UK, pp. 1–31.
9. Gaynutdinov,T.I., Neumann,R.D. and Panyutin,I.G. (2008) Structural polymorphism of intramolecular quadruplex of human telomeric DNA: effect of cations, quadruplex-binding drugs and flanking sequences. *Nucleic Acids Res.*, **36**, 4079–4087.
10. Phan,A.T., Kuryavyi,V., Luu,K.N. and Patel,D.J. (2007) Structure of two intramolecular G-quadruplexes formed by natural human telomere sequences in K^+ solution. *Nucleic Acids Res.*, **35**, 6517–6525.
11. Huppert,J.L. (2008) Four-stranded nucleic acids: structure, function and targeting of G-quadruplexes. *Chem. Soc. Rev.*, **37**, 1375–1384.
12. Webba da Silva,M. (2007) Geometric formalism for DNA quadruplex folding. *Chemistry*, **13**, 9738–9745.
13. Webba da Silva,M., Trajkovski,M., Sannohe,Y., Ma'ani Hessari,N., Sugiyama,H. and Plavec,J. (2009) Design of a G-quadruplex topology through glycosidic bond angles. *Angew Chem. Int. Ed. Engl.*, **48**, 9167–9170.
14. Neidle,S. and Parkinson,G. (2002) Telomere maintenance as a target for anticancer drug discovery. *Nat. Rev. Drug. Discov.*, **1**, 383–393.
15. Mergny,J.-L., Riou,J.-F., Mailliet,P., Teulade-Fichou,M.-P. and Gilson,E. (2002) Natural and pharmacological regulation of telomerase. *Nucleic Acids Res.*, **30**, 839–865.
16. Hurley,L.H. (2002) DNA and associated processes as targets for cancer therapy. *Nat. Rev. Cancer*, **2**, 188–200.
17. Zahler,A.M., Williamson,J.R., Cech,T.R. and Prescott,D.M. (1991) Inhibition of telomerase by G-quartet DNA structures. *Nature*, **350**, 718–720.
18. Zaug,A.J., Podell,E.R. and Cech,T.R. (2005) Human POT1 disrupts telomeric G-quadruplexes allowing telomerase extension in vitro. *Proc. Natl Acad. Sci. USA*, **102**, 10864–10869.
19. Lipps,H.J. and Rhodes,D. (2009) G-quadruplex structures: in vivo evidence and function. *Trends Cell Biol.*, **19**, 414–422.
20. Simonsson,T., Pecinka,P. and Kubista,M. (1998) DNA tetraplex formation in the control region of c-myc. *Nucleic Acids Res.*, **26**, 1167–1172.
21. Siddiqui-Jain,A., Grand,C.L., Bearss,D.J. and Hurley,L.H. (2002) Direct evidence for a G-quadruplex in a promoter region and its targeting with a small molecule to repress c-MYC transcription. *Proc. Natl Acad. Sci. USA*, **99**, 11593–11598.
22. Dapic,V., Bates,P.J., Trent,J.O., Rodger,A., Thomas,S.D. and Miller,D.M. (2002) Antiproliferative activity of G-quartet forming oligonucleotides with backbone and sugar modifications. *Biochemistry*, **41**, 3676–3685.
23. Bates,P.J., Kahlon,J.B., Thomas,S.D., Trent,J.O. and Miller,D.M. (1999) Antiproliferative Activity of G-rich Oligonucleotides Correlates with Protein Binding. *J. Biol. Chem.*, **274**, 26369–26377.
24. Teng,Y., Girvan,A.C., Casson,L.K., Pierce,W.M. Jr, Qian,M., Thomas,S.D. and Bates,P.J. (2007) AS1411 alters the localization of a complex containing protein arginine methyltransferase 5 and Nucleolin. *Cancer Res.*, **67**, 10491–10500.

25. Lane,A.N., Chaires,J.B., Gray,R.D. and Trent,J.O. (2008) Stability and kinetics of G-quadruplex structures. *Nucleic Acids Res.*, **36**, 5482–5515.
26. Chang,C.-C., Chien,C.-W., Lin,Y.-H., Kang,C.-C. and Chang,T.C. (2007) Investigation of spectral conversion of d(TTA GGG)$_4$ and d(TTAGGG)$_{13}$ upon potassium titration by a G-quadruplex recognizer BMVC molecule. *Nucleic Acids Res.*, **35**, 2846–2860.
27. Luu,K.N., Phan,A.T., Kuryavyi,V., Lacroix,L. and Patel,D.J. (2006) Structure of the Human Telomere in K^+ Solution: An Intramolecular (3+1) G-Quadruplex Scaffold. *J. Am. Chem. Soc.*, **120**, 9965–9970.
28. Phan,A.T. and Patel,D.J. (2003) Two-repeat human telomeric d(T AGGGTTAGGGT) sequence forms interconverting parallel and antiparallel G-quadruplexes in solution: distinct topologies, thermodynamic properties, and folding/unfolding kinetics. *J. Am. Chem. Soc.*, **125**, 15021–15027.
29. Wang,Y. and Patel,D.J. (1993) Solution structure of the human telomeric repeat d[AG3(T2AG3)3] G-tetraplex. *Structure*, **1**, 263–282.
30. Li,J., Correia,J.J., Wang,L., Trent,J.O. and Chaires,J.B. (2005) Not so crystal clear: the structure of the human telomere G-quadruplex in solution differs from that present in a crystal. *Nucleic Acids Res.*, **33**, 4649–4659.
31. Parkinson,G.N., Lee,M.P.H. and Neidle,S. (2002) Crystal structure of parallel quadruplexes from human telomeric DNA. *Nature*, **417**, 876–880.
32. Rosu,F., Gabelica,V., Poncelet,H. and De Pauw,E. (2010) Tetramolecular G-quadruplex formation pathways studied by electrospray mass spectrometry. *Nucleic Acids Res.*, **38**, 5217–5225.
33. Haider,S.M. and Neidle,S. (2010) Molecular modeling and simulation of G-quadruplexes and quadruplex-ligand complexes. *Methods Mol. Biol.*, **608**, 17–37.
34. Collie,G.W., Haider,S.M., Neidle,S. and Parkinson,G.N. (2010) A crystallographic and modelling study of a human telomeric RNA (TERRA) quadruplex. *Nucleic Acids Res.*, **38**, 5569–5580.
35. Antonacci,C., Chaires,J.B. and Sheardy,R.D. (2007) Biophysical characterization of the human telomeric (TTAGGG)$_4$ repeat in a potassium solution. *Biochemistry*, **46**, 4654–4660.
36. Miyoshi,D., Nakao,A. and Sugimoto,N. (2003) Structural transition from antiparallel to parallel G-quadruplex of d(G4T4G4) induced by Ca^{2+}. *Nucleic Acids Res.*, **31**, 1156–1163.
37. Mergny,J.L., Li,J., Lacroix,L., Amrane,S. and Chaires,J.B. (2005) Thermal difference spectra: a specific signature for nucleic acid structures. *Nucleic Acids Res.*, **33**, e138.
38. Mergny,J.-L., Phan,A.-T. and Lacroix,L. (1998) Following G-quartet formation by UV-spectroscopy. *FEBS Letters*, **435**, 74–78.
39. Olsen,C.M., Gmeiner,W.H. and Marky,L.A. (2006) Unfolding of G-quadruplexes: Energetic and ion and water contribution of G-Quartet stacking. *J. Phys. Chem. B*, **110**, 6962–6969.
40. Olsen,C.M. and Marky,L.A. (2010) Monitoring the temperature unfolding of G-quadruplexes by UV and circular dichroism spectroscopies and calorimetry techniques. *Methods Mol. Biol.*, **608**, 147–158.
41. Ambrus,A., Chen,D., Dai,J., Bialis,T., Jones,R.A. and Yang,D. (2006) Human telomeric sequence forms a hybrid-type intramolecular G-quadruplex structure with mixed parallel/antiparallel strands in potassium solution. *Nucleic Acids Res.*, **34**, 2723–2735.
42. Xu,Y., Noguchi,Y. and Sugiyama,H. (2006) The new models of the human telomere d[AGGG(TTAGGG)$_3$] in K^+ solution. *Bioorg. Med. Chem.*, **14**, 5584–5591.
43. Lee,J.Y., Yoon,J., Kihm,H.W. and Kim,D.S. (2008) Structural Diversity and Extreme Stability of Unimolecular Oxytricha nova Telomeric G-Quadruplex. *Biochemistry*, **47**, 3389–3396.
44. Miura,T., Benevides,J.M. and Thomas,G.J. Jr (1995) A phase diagram for sodium and potassium ion control of polymorphism in telomeric DNA. *J. Mol. Biol.*, **248**, 233–238.
45. Mergny,J.-L. and Lacroix,L. (1998) Kinetics and thermodynamics of i-DNA formation: phosphodiester versus modified oligodeoxynucleotides. *Nucleic Acids Res.*, **26**, 4797–4803.
46. Plavec,J. and Cevec,M. (2005) Role of Loop Residues and Cations on the Formation and Stability of Dimeric DNA G-Quadruplexes. *Biochemistry*, **44**, 15238–15246.
47. Bardin,C. and Leroy,J.L. (2007) The formation pathway of tetramolecular G-quadruplexes. *Nucleic Acids Res.*, **36**, 477–488.
48. Prislan,I., Lah,J. and Vesnaver,G. (2008) Diverse polymorphism of G-quadruplexes as a kinetic phenomenon. *J. Am. Chem. Soc.*, **130**, 14161–14169.
49. Cantor,C.R., Warshaw,M.M. and Shapiro,H. (1970) Oligonucleotide interactions. III. Circular dichroism studies of the conformation of deoxyoligonucleotides. *Biopolymers*, **9**, 1059–1077.
50. Jin,R., Gaffney,B.L., Wang,C., Jones,R.A. and Breslauer,K.J. (1992) Thermodynamics and structure of a DNA tetraplex: A spectroscopic and calorimetric study of the tetramolecular complexes of d(TG3T) and d(TG3T2G3T). *Proc. Natl Acad. Sci. USA*, **89**, 8832–8836.
51. Smirnov,I. and Shafer,R.H. (2000) Effect of loop sequence and size on DNA aptamer stability. *Biochemistry*, **39**, 1462–1468.
52. Ren,J., Qu,X., Trent,J.O. and Chaires,J.B. (2002) Tiny telomere DNA. *Nucleic Acids Res.*, **30**, 2307–2315.
53. Petraccone,L., Pagano,B., Esposito,V., Randazzo,A., Piccialli,G., Barone,G., Mattia,C.A. and Giancola,C. (2005) Thermodynamics and kinetics of PNA-DNA quadruplex-forming chimeras. *J. Am. Chem. Soc.*, **127**, 16215–16223.
54. Vorlíčková,M., Chládková,J., Kejnovská,I., Fialová,M. and Kypr,J. (2005) Guanine tetraplex topology of human telomere DNA is governed by the number of (TTAGGG) repeats. *Nucleic Acids Res.*, **33**, 5851–5860.
55. Kaushik,M., Bansal,A., Saxena,S. and Kukreti,S. (2007) Possibility of an Antiparallel (Tetramer) Quadruplex Exhibited by the Double Repeat of the Human Telomere. *Nucleic Acids Res.*, **46**, 7119–7131.
56. Lu,M., Guo,Q. and Kallenbach,N.R. (1993) Thermodynamics of G-Tetraplex formation by telomeric DNAs. *Biochemistry*, **32**, 598–601.
57. Rujan,I.N., Meleney,J.C. and Bolton,P.H. (2005) Vertebrate telomere repeat DNAs favor external loop propeller quadruplex structures in the presence of high concentrations of potassium. *Nucleic Acids Res.*, **33**, 2022–2031.
58. Kypr,J., Kejnovská,I., Renčiuk,D. and Vorlíčková,M. (2009) Circular dichroism spectroscopy and conformational properties of DNA. *Nucleic Acids Res.*, **37**, 1713–1725.
59. Press,W.H., Flannery,B.P., Teukolsky,S.A. and Vetterling,W.T. (1992) *Numerical Recipies in C++*. Cambridge University Press, Oxford, pp. 650–694.
60. Drobnak,I., Vesnaver,G. and Lah,J. (2010) Global thermodynamic analysis of reversible unfolding processes. *J. Phys. Chem. B*, **114**, 8713–8722.